

Active Pixel Sensors on High-Resistivity Silicon and Their Readout

W. Chen, G. De Geronimo, Z. Li, P. O'Connor, V. Radeka, P. Rehak, G. C. Smith, and B. Yu

Abstract—The concept of X-ray active matrix pixel sensor (XAMPS) is introduced. XAMPSs are direct illumination, position sensitive X-ray detectors with the possibility of containing 1 000 000 pixels. They count the number of diffracted X-rays in each pixel by measuring the total charge released by converted X-rays in the body of the sensor. Readout is accomplished with a relatively small number of channels equal to the square root of the number of pixels. The estimated readout time can be about 1 ms. Noise of the readout electronics can be so low that practically no additional fluctuations in the number of incident X-rays per pixel are added and, therefore, the XAMPS performance is very close to that of an ideal detector for X-ray crystallography.

Index Terms—Active pixel sensors, protein crystallography, silicon radiation detectors, X-ray imaging.

I. INTRODUCTION

IN RECENT years, structural studies in X-ray protein crystallography have been pursued overwhelmingly with image plates (IPs) and scintillator/CCD detectors (SCCDs). These devices are available almost exclusively from commercial vendors and have satisfied some of the demands of crystallographers during this time. The SCCD is now much more widely used than the IPs. The SCCD, however, is not an optimum device for synchrotron work. The scintillator suffers from “blooming” and the fiber-optic taper coupling scintillator to CCD exhibits nonuniformity. Most importantly, long CCD readout time (seconds) requires that beam-line shutters be closed for a significant percentage of an experiment’s duration. Structural biologists are constantly looking for an improved detector to reduce experiment time and improve accuracy.

We describe a new detector for X-ray protein crystallography. We call it the *X-ray active matrix pixel sensor* (XAMPS). Shown schematically in Fig. 1, it is a silicon pixel array detector with matrix readout facilitated by integrated junction field effect transistor (JFET) switches. The XAMPS is conceptually similar to two other imaging devices: the CMOS passive pixel sensor used for visible light imaging [1], [2] and the active-matrix flat panel imager (AMFPI) [3], [4], which has applications in both visible light and X-ray imaging. CMOS pixel sensor detectors are monolithic imaging devices fabricated on standard digital CMOS processes. They use the shallow p–n junctions native to CMOS technology with MOSFET transistors to make arrays of pixels and, in contrast to CCDs, are individually addressable

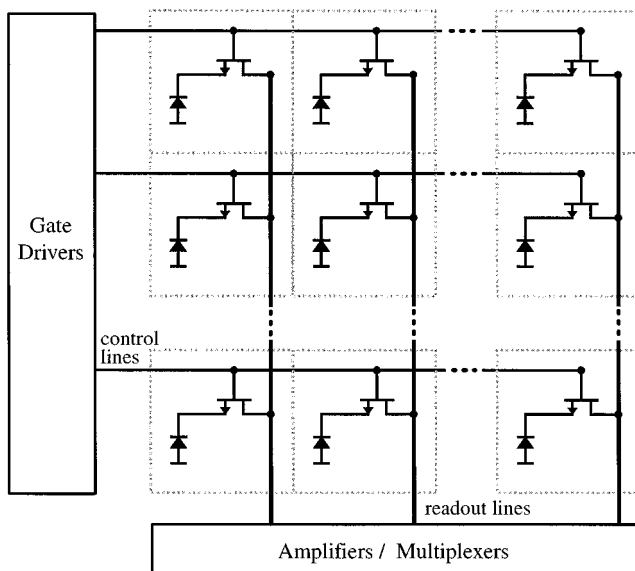


Fig. 1. Electronic equivalent circuit of XAMPS detector with peripheral electronics.

with readout performed line by line. Pixel sensors fabricated in modern submicrometer CMOS can contain over 10^6 pixels in chips of about 1 cm^2 , but they have poor sensitivity to X-rays because of the limited junction depth of CMOS.

The AMFPI detector uses a matrix of thin-film transistors (TFTs) on a large glass flat panel as switches to control the readout of a photosensitive layer. The AMFPI can be used as an X-ray detector if the photosensitive layer is directly converting (e.g., a-Se [5]) or if a scintillator layer is coupled to a visible-light sensing layer like a-Si [6].

The XAMPS detector was conceived from the start as a device that addresses the needs of protein crystallography. It combines attractive features of several technologies originating in other fields (visible light imaging, high-energy particle tracking). The main features of XAMPS are as follows:

- like the CMOS active pixel sensor, it uses integrated switch transistors and has fast readout;
- like the AMFPI, it is sensitive to X-ray energies in the range of interest to crystallography and can be made in large sizes;
- like the CCD, it has 100% fill factor and low noise (around 1 quantum equivalent);
- like the DEPFET [7], it uses direct-converting high-resistivity silicon as a starting material and adds monolithically integrated JFETs for matrix readout;
- like the various pixel array detectors (PADs) [8], which require bump-bonded readout electronics on each and every

Manuscript received November 21, 2001; revised February 25, 2002. This work was supported by the U.S. Department of Energy under Contract DE-AC02-98CH10886.

The authors are with the Brookhaven National Laboratory, Upton, NY 11973 USA (e-mail: rehak@bnl.gov).

Publisher Item Identifier S 0018-9499(02)06100-2.

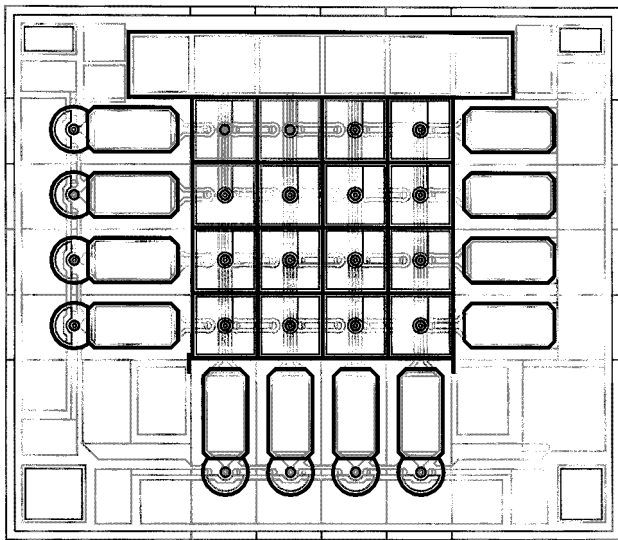


Fig. 2. The electronic side of a test XAMPS having 16 pixels arranged in four rows and four columns. Vertical lines connected to the bonding pads at the bottom of the array are the readout lines. Each line is bonded to a charge sensitive preamplifier. The horizontal lines are terminated with bonding pads on the left-hand side as well as on the right-hand side of the array. These lines are bonded to the switch controlling electronics.

pixel, the XAMPS can resolve single photons and has dynamic range of more than 10^4 .

Among all the detectors optimized for X-ray energies of interest to crystallography (typically 12 keV), only the XAMPS combines 100% fill factor, single photon sensitivity, readout speed fast enough to accept the full intensity of third-generation light sources without mechanical shuttering, good combination of pixel size and overall area, moderate number of readout channels, tolerance to radiation, and monolithic assembly.

II. X-RAY ACTIVE PIXEL SENSOR ON HIGH-RESISTIVITY SILICON

One side of the silicon wafer comprising XAMPS is subdivided into a large number of pixels, each of which is in principle a classical semiconductor diode detector. In crystallography, the energy of incident X-rays is known. And the exact time of incidence of individual particles is of no interest. The number of incident X-ray photons on each pixel during a time frame forms the information of interest (picture) and fluctuates according to the Poisson statistics.

Fig. 2 shows the pixelized side of a test XAMPS with 16 pixels arranged in four rows and four columns. Vertical lines connected to the bonding pads at the bottom of the array are the readout lines and each line is bonded to an external charge sensitive preamplifier. The horizontal lines control the gates of the integrated JFET switches and are terminated with bonding pads on the left-hand side (LHS) of the array (as well as on the right-hand side (RHS), a redundancy in this prototype design).

The device uses direct conversion of the X-ray in silicon. Incident X-rays create electric charge directly within the active volume of the sensor, in contrast to an indirect detection system where X-rays, after stopping in a scintillator, are converted into a light signal, which is then registered in a silicon based position sensitive light detector (CCD). For a detection efficiency

above 80% the thickness d of the active silicon should be at least equal to twice the absorption length. For 12 keV, a preferred energy for crystallography, $\lambda = 200 \mu\text{m}$ and therefore d should be $\geq 400 \mu\text{m}$. To achieve this the detector has to be made on high-resistivity silicon where full depletion can be reached at reasonable applied voltages (100 to 200 V). The fully depleted detector has all of the silicon active and all electrons produced by photon conversions are delivered to the pixels (fill factor equals one).

The principle of operation of XAMPS is very similar to that of CMOS pixel sensors. The most important differences are the silicon material and the thickness of the active area. Fig. 3 shows a three-dimensional (3-D) schematic of a single pixel in an XAMPS consisting of a 300–500 μm thick, high-resistivity (several $\text{k}\Omega\cdot\text{cm}$) n-type silicon layer. The volume of silicon is fully depleted of majority carriers (electrons) by applying relatively large negative potential (-100 V to -200 V) to the rectifying junction at the bottom. All structures on the top are biased at or close to ground potential. The electric field within the bulk of the XAMPS is perpendicular to the planar surfaces of the wafer. The preferred entrance side for incident X-rays is the bottom, with its continuous shallow rectifying junction. All electrons produced by conversion of X-rays are swept toward the top of the sensor, preserving the position information of the conversion point. After reaching the top side of the pixel the signal electrons remain there and are stored until being removed during the readout cycle.

The cylindrical structure in the top middle of the pixel on Fig. 3 is an integrated JFET switch. The JFET switch connects or disconnects the charge collecting electrode to the readout line passing above the pixel. Each readout line ends at the edge of the detector with a bonding pad for the connection to the corresponding front-end electronics. The first stage of the readout chain is a charge sensing amplifier with a low-input impedance, which removes completely the charge from the input node and transports it to the feedback capacitor. The integrated JFETs are intrinsically radiation hard [9]. The readout electronics is located at the periphery and is not irradiated during exposure. Hence, any convenient technology may be used without regard to radiation tolerance. There is no need for high stopping power layers or upset-tolerant circuit design as in PAD detectors.

The readout sequence of this XAMPS is the following. Assuming that all pixels have been cleared of any accumulated charge, switches in all pixels are open and the detector is exposed to the X-rays. The charge from the converted X-rays is accumulated in the respective pixels and the quantity of the accumulated charge is proportional to the number of incident X-ray photons in every pixel. The readout is carried out for every pixel in a horizontal control line simultaneously. The control voltage brings all field effect transistor (FET) switches on the line into the ON state and the charges from all pixels within this row are transferred through the vertical readout lines into the charge sensing preamplifiers. Thus, all pixels within one row (in our illustrative case of Fig. 2 four amplifiers) are read in parallel. The charge transfer from the pixel to the readout electronics resets all pixels within that row making it ready for the subsequent charge integration. After finishing the reading of one row, the next row is selected. For the detector shown in Fig. 2, four rows have to

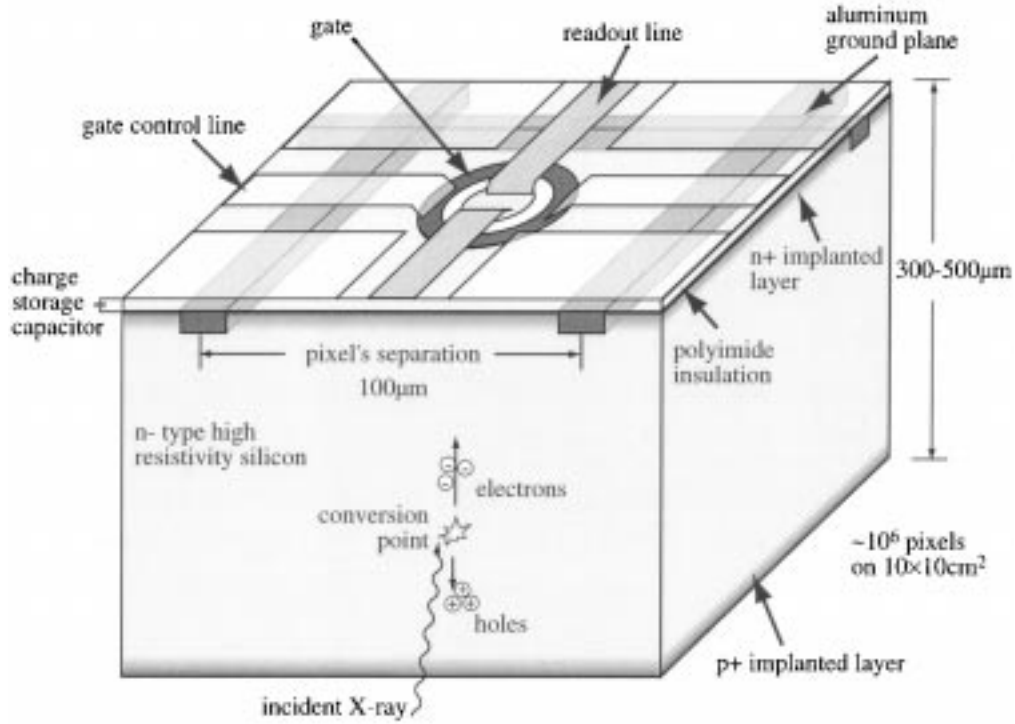


Fig. 3. A schematic view of the structure of a single pixel in an XAMPS.

be read out to obtain a complete frame of the XAMPS. A practical XAMPS may have a number of rows and columns close to 1000. Such a detector has 1 000 000 pixels, but needs only 1000 readout channels and 1000 line drivers to provide complete information.

It will be shown that the resolution of the proposed sensor can approach the resolution of an ideal sensor. Thus, selection of the detector architecture and its readout electronics to provide this excellent performance in a practical and robust system is justified.

III. COMPARISON OF THE XAMPS WITH AN IDEAL DETECTION SYSTEM

Let us define the ideal detector for the X-ray crystallography. This detector would count the *true* number (100% efficiency) of incident X-rays within each pixel, at any counting rate with a point-spread function less than the pixel size. The dynamic range of an ideal detector is not limited. The active pixel detector made on high-resistivity silicon can have a square pixel with dimension around 100-μm, matching well the beam size. Each pixel accumulates the total charge produced by conversion of N X-ray photons. The number of incident X-rays N is deduced from the measurement of the total charge. The average charge \bar{Q} produced by one X-ray photon equals

$$\bar{Q} = q \cdot E/w \quad (1)$$

where q is an elementary charge, E is the energy of the incident X-ray in eV and $w = 3.6$ eV is the average energy needed to produce one electron-hole pair in silicon. Not all X-rays produce exactly the same average charge and the collected charge from

one fully contained X-ray fluctuates according to a Gaussian distribution with root mean square (rms) σ_Q equal to

$$\sigma_Q = q \cdot \sqrt{F \cdot E/w} \quad (2)$$

where F is the Fano factor, equal to a constant between 0.1 and 0.2 for a good silicon detector. Equation (1) shows that each 12-keV X-ray produces about 3300 electron charges in the silicon. Equation (2) shows that the fluctuations in the produced charge are smaller than the fluctuation corresponding to the production of 3300 independent electron charges. The proposed method measures the total charge released by N converted X-rays. $Q_{\text{tot}} = \sum_{i=1}^N Q_i$. In this summation each Q_i fluctuates according to (2) and the number of converted X-rays fluctuates according to the Poisson statistics with the mean number \bar{N} . This is an example of a well-studied compound process [10] for which the mean value and variance are, respectively

$$\bar{Q}_{\text{tot}} = \bar{N} \cdot \bar{Q}; \quad \text{var}[Q_{\text{tot}}] = (\bar{Q})^2 \cdot \text{var}[N] + \bar{N} \cdot \text{var}[Q]. \quad (3)$$

Substituting into the expression for $\text{var}[Q_{\text{tot}}]$ of (3) from (1) and (2) we obtain

$$\text{var}[Q_{\text{tot}}] = (qE/w)^2 \cdot \bar{N} \cdot (1 + Fw/E). \quad (4)$$

We are interested in the number of X-rays measured by the charge integration method. To obtain the number of converted X-rays from the charge, we divide the measured charge by the mean charge produced by one X-ray, given by (1). Equations (3) and (4) thus give

$$\bar{N}_Q = \bar{N}; \quad \text{var}[N_Q] = \bar{N}(1 + Fw/E) \quad (5)$$

where \bar{N}_Q denotes the number of converted X-rays within a pixel measured by the charge integration method. From the LHS

of (5), we see that the integration method provides an unbiased estimate of the number of converted X-rays within a pixel. The RHS of (5) shows that the variance of the number of measured photons by the method is increased by a factor of $(1 + Fw/E)$ as compared to the Poissonian statistics of the incident X-rays. The numerical value of this factor for 12-keV X-rays and Fano factor of 0.2 is about $1 + 6 \times 10^{-5}$. This is a negligible increase. We can restate this result in a more conventional way. The relative error of the number of X-rays within a pixel measured by a charge integration method

$$\begin{aligned} \frac{\sqrt{\text{var}[N_Q]}}{\bar{N}_Q} &= \frac{\sqrt{\bar{N}(1 + 6 \times 10^{-5})}}{\bar{N}} \\ &= \sqrt{\frac{1 + 6 \times 10^{-5}}{\bar{N}}} = \sqrt{\frac{1 + 6 \times 10^{-5}}{\varepsilon \cdot \bar{N}_{\text{incident}}}} \quad (6) \end{aligned}$$

where we have introduced the average number of incident X-rays $\bar{N}_{\text{incident}}$ by the relation $\bar{N} = \varepsilon \cdot \bar{N}_{\text{incident}}$, where ε is the detection efficiency that is the probability of a conversion of an X-ray in the detector. The final expression on the RHS of (6) shows that, as far as the relative fluctuations in the number of X-rays detected by the charge integration method, the factor $(1 + Fw/E)$ decreases the efficiency of the detector. The increase in the relative fluctuations with the square root of the detection efficiency is present also for any nonideal counting method. Given the proximity of the value of $(1 + Fw/E)$ factor to 1 (for our values $(1 + Fw/E) = 1.00006$) it is much more important to keep the conversion efficiency high to approach the limit of an ideal detector by any method.

IV. CONSIDERATIONS FOR PRACTICAL DETECTORS

The charge integration method described above assumed no noise in the readout electronics and did not consider charges divided among several pixels. The noise of the electronics readout degrades the charge measurement. The loss of precision of X-ray counting can be compared with the precision of an ideal detector in the same spirit as the analysis above. The sharing of the charge among several pixels is a typical instrumentation effect completely absent in an ideal detector. We can compare the charge splitting in our detector with the charge splitting in different detectors and try to find a strategy to minimize its negative impact for the performance of our device. These two aspects, clearly separate in origin, have to be considered together in a practical detector.

The details of the readout electronics chain with the noise analysis will be described in a later publication. Here, we will justify the architecture of the detector having relatively long readout lines directly on the surface of the XAMPS. There are four vertical readout lines shown in Fig. 2. In a sensor with many more pixels, these lines are substantially longer and, consequently, have a larger capacitance to ground. The lines are part of the input node of the readout preamplifiers. More capacitance at the input means more series noise in the readout channel. For a practical sensor with many (several hundreds times several hundreds) pixels the capacitance of the line is close to 20 pF. This has to be compared to the capacitance of the pixel, which may be designed to be as low as 0.5 pF. XAMPS can support a line

capacitance as high as 20 pF while achieving equivalent noise charge (ENC) about 1000 electrons for the measurement time of about 1 μ s. As calculated above, a single 12-keV X-ray delivers a charge of about 3300 electrons. Here, we see that our direct illumination sensor can function with much higher level of ENC when compared to ENC of an indirect sensor. In an indirect detection system the X-ray energy is converted into, say, scintillating light and this light is brought to a silicon detector. The charge produced in the indirect illumination detector by one 12-keV X-ray is only several electrons. Our signal is about three orders of magnitude larger than the signal in those systems and our noise is only slightly more than two orders of magnitude larger. XAMPS thus has the signal to noise ratio a factor ten higher than that of an indirect system.

Having a relatively large charge signal for each detector the required dynamic range pushes the charge storage capability of the individual pixel to its limit. Preliminary studies indicate that the maximal capacitance of a pixel with 100- μ m linear size is about 2.5 pF. The maximal potential excursion of the charge-collecting electrode within a pixel is about 2 V. Therefore, the maximal charge that can be stored within a pixel before it starts leaking out is 5 pC, which is equivalent to the charge produced by 10^4 incident 12-keV X-rays. The capacitance of the pixel, formed by a p-i-n junction in silicon, may not be constant within this dynamic range. However, all charge from the pixel is transferred during the readout time to the input stage of the electronics (feedback capacitor of the preamplifier) and the variations of the pixel capacitance are of no consequence.

V. MULTIPLE READOUT CYCLES PER SINGLE FRAME

A typical XAMPS may have of the order of 1000×1000 pixels. If one line of the pixel array is read within 1 μ s, the total readout time of the detector is about 1 ms. Depending on the desired frame rate of an experiment, the total charge on each pixel can be summed from multiple read cycles. It is possible to find a readout sequence such that the most important noise contribution, the equipartition noise associated with the pixel cell capacitance (usually referred to as the kTC noise), does not depend on the number of readout cycles when all read charges are summed together. This is clearly the preferred readout scheme for pixels exposed to a high intensity of the X-rays. Details of this readout scheme will be described in a follow-up paper.

The maximum count rate capability of the current XAMPS design is 10^4 converted 12-keV X-rays per pixel per 1 ms, or an effective rate of 10^7 per pixel/s. The maximum count rate per pixel in today's highest intensity light sources is about 10^5 /s. The more powerful synchrotron light sources under construction may deliver beam intensities two orders of magnitude higher, reaching the limit of the current XAMPS design. It should be stressed that, at this rate there is NO COUNTING LOSS. By contrast, all counting systems are characterized by a dead time t_p associated with the counting of each photon. The maximum counting rate is usually given as $1/t_p$. However, at this rate there is significant counting loss due to the random arrival of the photons.

For pixels with a low X-ray count, a different method can be used to avoid an increase of the series noise with multiple

readout cycles. Since the noise of an individual readout is much smaller than the charge delivered by a conversion of a single photon, we can round the number of the detected X-rays within each pixel to an integer number. For example, if the charge read from a pixel corresponds to 4.2 X-rays, we can round it to four X-rays, thus eliminating the noise contribution. In this way we are counting a real number of converted X-rays and excluding the contribution of the noise by taking advantage of the quantization of the number of incident X-rays.

VI. PRODUCTION OF THE XAMPS ON HIGH-RESISTIVITY SILICON

Fabrication of XAMPS is more demanding than producing a standard pixel detector. The two additional features contributing to the complexity of the production are: 1) presence of 10^4 to 10^6 switching transistors integrated on high resistivity silicon of the sensor and 2) the second layer of metallization running above a 3- μm -thick layer of polyimide.

The switching transistor integrated in every pixel of XAMPS is very similar to the single sided field effect transistor (SSJFET) [11] with only slightly different geometry of the deep implanted channel and back gate regions due to different requirements of the transistor. The OFF resistance of the XAMPS transistor has to be greater than about $10^{13} \Omega$. Moreover, the area of the transistor permanently connected to the readout line must not receive any signal electrons during the integration time of the pixel. This protection was achieved with a deep ($\sim 1 \mu\text{m}$) boron implant at the central part of the transistor. The electric field created by the negative charge of ionized acceptors repels signal electrons, creating an electron “umbrella” over the central region of the transistor. The switching parameters of the transistor must be reasonably uniform over the $6 \times 6 \text{ cm}^2$ detector area, and the process sufficiently defect free to allow an adequate yield. On the other hand, the transistor is not used for the signal amplification and there is no requirement for the high output impedance of the transistor.

The second metallization layer was a new technological step. The lines of the second metal layer are running long distances (several cm) on a semiconductor scale, at a separation of 3 μm from the first layer to keep the capacitance of the readout lines small. We used polyimide as the dielectric material between two metal layers. It has a low dielectric constant and a relatively low loss. A typical gate controlling line has about 2000 contacts between the two metal layers. After some initial problems, the existing prototypes achieve almost 100% connectivity between the two metal layers. About 20 000 contacts were checked as 80 measurements of group of 256 contacts connected in series. No missing connection was found.

Fig. 4 shows a microphotograph of the area of pixels of a prototype XAMPS. Vertical and horizontal lines are readily visible being on the upper metal layer. There is a transistor in each crossing of vertical (readout) and horizontal (control) lines. Boundaries among pixels are less visible because they are implemented under the upper metal layer.

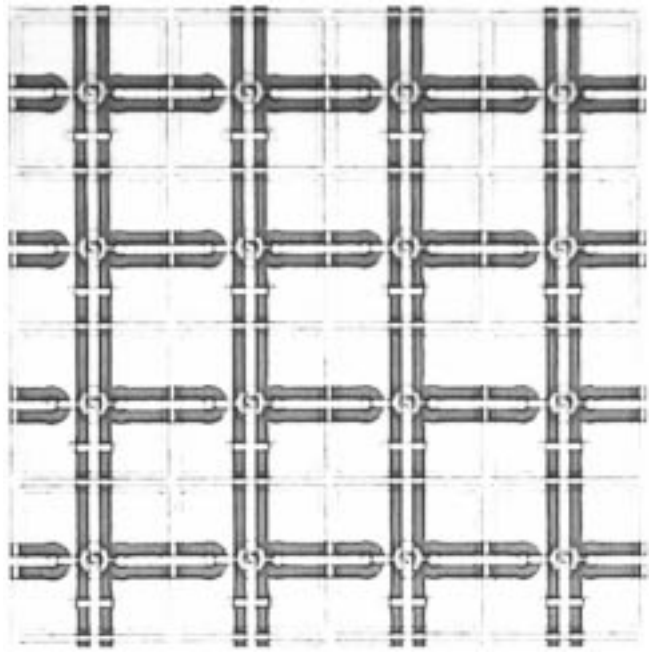


Fig. 4. A microphotograph of several pixels of a prototype XAMPS.

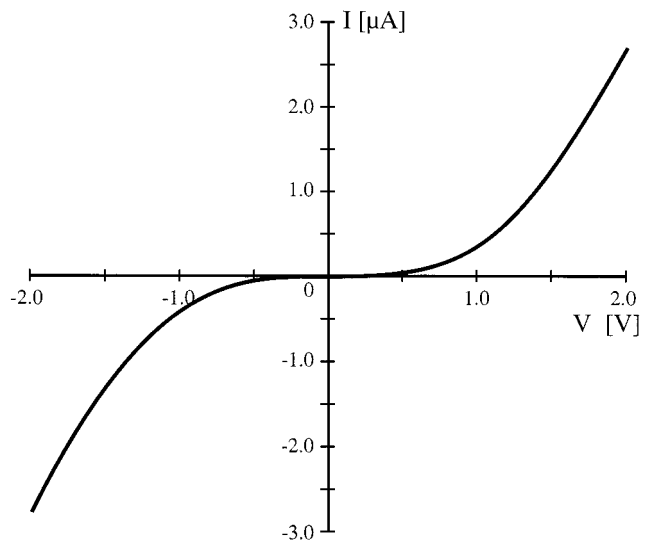


Fig. 5. IV characteristics of two ohmic contacts in series—one from aluminum at the top of silicon into the phosphorus implanted silicon and the second contact in the opposite direction.

VII. TEST RESULTS

Several wafers with the prototype of XAMPS were designed, produced, and are currently under extensive testing. As mentioned above, the problems with the contacts between the two metal layers was solved. An unexpected problem was found with the dose and the energy of the implanted n-type contact (phosphorus) into the n-type silicon to form a simple ohmic contact. Fig. 5 shows the IV characteristics of two ohmic contacts in series—one from aluminum at the top of silicon into the phosphorus implanted silicon and the second contact in the opposite direction. A straight line is expected. The curve shown on Fig. 5 has a very flat part at the origin of the coordinate system.

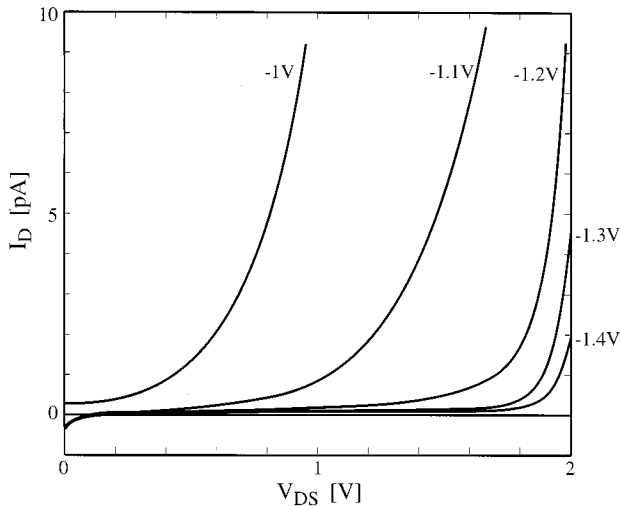


Fig. 6. Characteristics of the transistor for a gate voltage close to or at the pinch-off voltage, demonstrating the high open switch resistance ($10^{13} \Omega$) achieved in the XAMPS. The voltage of the back side of the detector was -140 V.

It means that the resistance of the ohmic contact is very large, in our case several tens of mega ohms. In the design of XAMPS, one terminal of the JFET switch is connected to the readout lines. Such a high value of the contact resistance would increase the transfer time of the charge from the pixel to the readout line. The increase of the transfer time would result in an unacceptable increase of the readout time of the XAMPS. It is interesting to note that the problem of high contact resistance was not present in an older technology. The measurement of identical test structure on an older wafer as the structure measured to produce the curve on Fig. 5 shows a simple straight line passing through the origin of the I - V graph. The slope of this line corresponds to a resistance of about $5 \text{ k}\Omega$. The value of the resistance is about four orders of magnitude smaller than the value of the resistance at the origin of the curve shown in Fig. 5. A few new wafers where we returned to the old and proven technological steps are in production.

Fig. 6 shows a few characteristics of the transistor for the value of the gate voltage close or at the pinch-off voltage. Pinch-off voltage corresponds to an open switch. Drain current as a function of the voltage between the source and the drain is being presented. The lowest curve out of the series was taken at the value of the gate voltage of -1.4 V. The remaining drain current at the source to drain voltage of 1 V is less than 0.1 pA. This value translates to the remaining resistance of on open switch more than $10^{13} \Omega$, which is sufficiently high. The

full spread of the gate voltage for which the high value of the resistance of an open switch was reached is about 0.2 V. At a gate voltage of -0.8 V or higher, the resistance of the transistor is in the order of $10^8 \Omega$, limited by the problem of the nonohmic contact. A realization of a transistor with such a high value of the resistance in an open state of the switch was considered one of the most difficult tasks of the detector design and production.

VIII. CONCLUSION

A concept of a new detector for the protein crystallography XAMPS was introduced. The prototype of the detector was designed, produced and is presently being tested. The most demanding requirement of a very high resistivity of an open switch was verified experimentally. A problem with a nonohmic characteristics of a nominal ohmic contact was found. The problem was traced to incorrect parameters of a phosphorus implant and a new production of XAMPS with the corrected phosphorus implant was started. The test results known up to now indicate that there is no principal obstacle to produce XAMPS with the required performance.

REFERENCES

- [1] M. Schanz, C. Nitta, A. Bussmann, B. Hosticka, and R. K. Wertheimer, "A high dynamic range CMOS image sensor for automotive applications," *IEEE J. Solid-State Circuits*, vol. 35, pp. 932–938, July 2000.
- [2] E. R. Fossum, "CMOS image sensors: Electronic camera-on-a-chip," *IEEE Trans. Electron Devices*, vol. 44, pp. 1689–1698, Oct. 1997.
- [3] J.-P. Moy, "Large area X-ray detectors based on amorphous silicon technology," *Thin Solid Films*, vol. 337, pp. 213–221, 1999.
- [4] R. A. Street, "High performance amorphous silicon image sensor arrays," *J. Non-Cryst. Solids*, vol. 1306, pp. 227–230, 1998.
- [5] W. Zhao, J. Law, D. Waechter, Z. Huang, and J. A. Rowlands, "Digital radiology using active matrix readout of amorphous selenium: Detectors with high voltage protection," *Med. Phys.*, vol. 25, pp. 539–549, 1998.
- [6] S. Ross, G. Zentai, K. S. Shah, R. W. Alkire, I. Naday, and E. M. Westbrook, "Amorphous silicon, semiconductor X-ray converter detectors for protein crystallography," *Nucl. Instrum. Methods*, vol. A399, pp. 38–50, 1997.
- [7] P. Fischer *et al.*, "First operation of a pixel imaging matrix based on DEPFET pixels," *Nucl. Instrum. Methods*, vol. A451, pp. 651–656, 2000.
- [8] S. L. Barna, J. A. Shepherd, M. W. Tate, R. L. Wixted, E. F. Eikenberry, and S. M. Gruner, "Characterization of a prototype pixel array detector (PAD) for use in microsecond framing time-resolved x-ray diffraction studies," *IEEE Trans. Nucl. Sci.*, vol. 44, pp. 950–956, 1997.
- [9] M. Citterio, J. Kierstead, S. Rescia, and V. Radeka, "Si-JFET devices and related noise behaviors under irradiation," *Nucl. Phys. B*, vol. 61B, pp. 526–531, 1998.
- [10] A. T. Bharucha-Reid, *Elements of the Theory of Markov Processes and Their Applications*. Mineola, NY: Dover, 1988, p. 441, appendix A, theorem A4.
- [11] V. Radeka *et al.*, "Design of a charge sensitive preamplifier on high resistivity silicon," *IEEE Trans. Nucl. Sci.*, vol. 35, pp. 155–159, 1988.